

Magnetic measurements of AGS experimental beam quadrupoles

G. T. Danby

December 1963

Collider Accelerator Department
Brookhaven National Laboratory

U.S. Department of Energy

USDOE Office of Science (SC)

Notice: This technical note has been authored by employees of Brookhaven Science Associates, LLC under Contract No. AT-30-2-GEN-16 with the U.S. Department of Energy. The publisher by accepting the technical note for publication acknowledges that the United States Government retains a non-exclusive, paid-up, irrevocable, world-wide license to publish or reproduce the published form of this technical note, or allow others to do so, for United States Government purposes.

DISCLAIMER

This report was prepared as an account of work sponsored by an agency of the United States Government. Neither the United States Government nor any agency thereof, nor any of their employees, nor any of their contractors, subcontractors, or their employees, makes any warranty, express or implied, or assumes any legal liability or responsibility for the accuracy, completeness, or any third party's use or the results of such use of any information, apparatus, product, or process disclosed, or represents that its use would not infringe privately owned rights. Reference herein to any specific commercial product, process, or service by trade name, trademark, manufacturer, or otherwise, does not necessarily constitute or imply its endorsement, recommendation, or favoring by the United States Government or any agency thereof or its contractors or subcontractors. The views and opinions of authors expressed herein do not necessarily state or reflect those of the United States Government or any agency thereof.

GTD/JWJ-2

BROOKHAVEN NATIONAL LABORATORY
Associated Universities, Inc.
Upton, L.I., New York

ACCELERATOR DEPARTMENT
(AGS)
Internal Report

MAGNETIC MEASUREMENTS OF AGS EXPERIMENTAL BEAM QUADRUPOLES

Gordon T. Danby & John W. Jackson

December 2, 1963

I. Introduction

This report summarizes the results of the magnetic measurements which have been taken on the AGS experimental beam quadrupoles. Results on the following types of magnets are included in this report:

Circular Quadrupoles 8Q24, 8Q48, 12Q30, 12Q60

Rectangular Quadrupoles RQ(6x24x36)

The first section of the report will describe the results obtained for the circular quadrupoles, while the second section will deal with the rectangular quadrupoles.

II. Circular Quadrupoles

In order to measure the harmonic content of the circular quadrupoles a harmonic coil was constructed; the mechanical design for this coil was done by B. DeVito; the theory and design of the coil will be described in a future report dealing with the general methods of measurement used.

The chief advantage of this device is that the centering of it in the magnet is not critical provided it remains rigid during the time of the measurement, i.e., it has a true axis of rotation. The only term effected by an error in centering is the dipole term; because of orthogonality relations, there is no effect on the other terms. A further advantage is that the effective radius of the coil is not critical, to first order, provided it is constant during the duration of the measurement. That is, one is measuring the true ratio of the terms at an effective radius which may be slightly different (say, .005") from the nominal. This results in a completely negligible error in the nonlinear coefficients which are already quite small for good quadrupoles. The device has a point coil for measuring the internal two-dimensional harmonic content and a long coil to give the integrated harmonic content in the ideal thick lens approximation.

The harmonic coil could in principle be calibrated to give absolute values, like those given in a previous report¹. However, the authors prefer to use it only to measure quadrupole nonlinearity. Absolute integral field and gradient values for all types of magnets are measured with one long coil device as indicated in the previous report¹. Figures 1 through 6 are taken from the previous report and the reader is referred to that report for an explanation of the curves.

From a knowledge of the four-pole symmetries involved, one can expand the quadrupole field in terms of 2θ , 6θ , 10θ , etc. There can also exist terms like 1θ , 3θ , 4θ , 5θ , 7θ , 8θ , etc. which are due to errors in the four-pole symmetry. Using the harmonic coil results to perform a harmonic analysis, one can obtain the coefficients of the various terms at the radius of the coil. The 1θ term (dipole) simply indicates the effective center of the magnet with the respect to the coil axis. The 3θ , 4θ , etc. terms are true error terms in the sense of field asymmetry. As one would expect the 3θ , 5θ , 7θ , etc. terms are almost zero. The 4θ term should be prominent if mechanical asymmetry exists since it corresponds, for example, to top to bottom asymmetry.

The harmonic content of one magnet of each type was measured as a function of current and the results are summarized in Table I. These measurements were taken with both long coil and point coil at low, medium and high fields as indicated in the table. The results are the ratios of the harmonic error field to the true quadrupole field at the nominally maximum radius (approximately $1/16''$ from the pole tip).

III. Discussion

Table I shows that the nonlinearity in the AGS beam quadrupoles is very small. The phase angles of all terms with respect to the 2θ phase is also considered in the harmonic analysis, and the relevant phases are given in Table II. The small deviations of the measured phase angles from the angles predicted by the four-pole symmetry indicate the high quality of the quadrupole field as well as the high accuracy of the measurement.

The ratio $4\theta/2\theta$, which represents the magnitude of the most likely nonlinear contribution due to mechanical asymmetries (octupole) compared to

the quadrupole field, is included in the table. Any errors in the measurement will also contribute to the coefficients. The magnitude of the $4\theta/2\theta$ result indicates that both the octupole aberration and measurement errors are negligible.

The high quality of the M.H. Blewett pole profile is indicated by the small internal, i.e., no end effects, nonlinearity. The variation in linearity with field strength is very small because of the parallel coil slots which provide wide based poles and keep any saturation effects on linearity to a minimum.

The integrated results contain the nonlinearity of both the internal field, and that of the ends in the thick lens approximation. By comparing the integrating coil and the point coil results for different ratios of magnet length to magnet diameter, one can see that the ends contribute significantly to the nonlinearity. In addition, the nonlinearities due to the truly three dimensional nature of the fields can contribute significantly to beam aberrations. This effect will be discussed in a more detailed report.

IV. Rectangular Quadrupoles

For the circular quadrupoles, the harmonic coil results give the terms (including the error terms) of a complete field expansion in the thick lens approximation. This is also true for any other magnet type with the appropriate symmetry, for example, sextupoles. However, the AGS rectangular quadrupoles have a 6" x 24" aperture for matching to the electrostatic beam separators and thus the field can best be described by measuring and fitting to an expansion in rectangular coordinates.

These quadrupoles, while excellent for the special purpose for which they were designed, have certain disadvantages compared to the conventional circularly symmetric quadrupoles, apart from the fact that they are less efficient from a power consumption point of view. The magnetic design is very simple (Fig. 7). For infinite permeability it is easily seen that a pure quadrupole field satisfies the boundary conditions. However, the actual location of the copper conductors is much more important in determining field nonlinearity than in the conventional circular quadrupoles where the poles chiefly determine the field. Since in practice iron tolerances can easily be held more than an order of magnitude better than the copper coil tolerances, the location of the coil becomes a quite important factor. Furthermore, in the circular quadrupoles the forces on the coils push them radially outward against the yoke and poles, which is a stable position. In the rectangular quadrupole the forces on the coils (Fig. 7) are pushing them toward the axes xx and yy as well as outwards against the core. This results in a strong distorting force on the coils. This effect was observed in all but one of the four rectangular quadrupoles tested, that is, the fields tended to "float" by a few tenths percent as a function of time. This is an unpleasant situation not only because the gradient or lens strength changes, but also the amount of nonlinearity produced changes. Such a distortion depends on water pressure, temperature, and torsion in the coil holding clamps, as well as the field strength, and is obviously difficult to cope with. With careful adjustment of torsion in the coil clamps and control of water temperature one should be able to improve the situation, and in any case the effect should be barely noticeable in a beam system.

Because of the limitation on precision outlined above, only measurements of the vertical component of field on the wide or horizontal (xx) symmetry plane were made. The azimuthal integral of the magnetic field was measured as a function of current and position on this plane. The nonlinearity in the gradient length is shown in Fig. 8 as a function of transverse distance along the horizontal symmetry plane, with current as a parameter. Gradient length is here defined as $\int [B(s) \cdot ds]_x/x$, i.e., the value of the field integral at location x on the horizontal symmetry plane divided by the value of x. Thus, in this terminology the gradient is not dB/dx except for a linear field. For each curve (Fig. 8) the values are relative only to the values at the aperture centerline.

From a knowledge of the symmetries one may expand the field on the horizontal symmetry plane as:

$$B_y = Gx + a'x^3 + bx^5 + \dots \quad (1)$$

Dividing (1) by x one obtains:

$$"G" = G (1 + ax^2 + bx^4 + \dots) \quad (2)$$

and $(ax^2 + bx^4)$ represents the relative nonlinearity as plotted in Fig. 8. The curves were fitted to an x^2 and x^4 expansion to an accuracy of 0.5% using the least squares method; the results are summarized in Table III.

TABLE III

B_T (Kg)	<u>a</u>	<u>b</u>
2.0	-2.905×10^{-4}	$+8.932 \times 10^{-7}$
8.5	-2.879	+8.853
15.0	-3.644	+13.206

For example, for $B_T = 2$ kg at $x = 10''$, the first nonlinear term (ax^2) gives -2.9% deviation from the pure quadrupole field (or gradient) and the second term (bx^4) gives +0.9%. The quality of the fit should be an indication of the validity of the assumption of only symmetrical aberrations. Strictly speaking, one would only see large asymmetrical terms on the xx axis if the phases happened to be right. However, since the aperture is large only for fairly small angles about this plane, a term which is not seen on the xx plane should not be appreciable at any positions off the axis.

Figure 9 gives the absolute integral of the field as a function of magnet current at the $x = 6''$ position. The hysteresis is about 0.2% and in a beam setup the desired field should be set on the down current cycle for the best reproducibility.

Figure 10 indicates the variation of L_B (magnetic length) as a function of current. The L_B 's are obtained by dividing $\int [B(s) \cdot ds]_{x=6''}$ by the internal, i.e., two dimensional, field at $x = 6''$ at a given current. Strictly speaking, one would get a slightly different L_B at some other value of x but $x = 6''$ is a mean position and L_B is a useless concept unless it is defined to hold for all positions. Secondly, L_B changes less than 0.5% as a function of magnet current so it is convenient to define one mean value of L_B from Fig. 10, say, $L_B = 42.30''$ and let all the variation in $\int [B(s) \cdot ds] (= BL_B)$ be in the field. This is a very good approximation since, for example, a thick lens 0.25% shorter in length and 0.25% higher in field will have negligibly different focal properties.

V. Discussion

Knowing L_B (Fig. 10) and the absolute value of the integral (Fig. 9) one can compute $B(x = 6")$ as a function of current. There now exists two approaches to constructing the field everywhere.

The most accurate in principle, is to use Table III to equate

$$B(x = 6") = "G" \times 6" = G \times 6 \left[1 + a (6)^2 + b (6)^4 \right]. \quad (3)$$

Figure 8 shows that the variation as a function of current is slow enough so that a very good fit could be made over the entire working range. The a and b terms correspond to the octupole and 12 pole aberrations respectively; their value off the axis could be established by substituting into a field expansion. Thus one would have a good description of the field everywhere based on the assumption that any unsymmetrical aberrations are small, as is indeed the case since the quality of the fit of the nonlinearities to $(ax^2 + bx^4)$ is excellent. This method will be covered more thoroughly in a more complete report on quadrupoles to follow; a simpler approach, to be described in the next section, appears to be quite adequate for the present purposes.

From Fig. 8 one can see that even at low fields there is no linear region, i.e., the statement $\left[B_y \right]_x = Gx$ is a very poor approximation except near the very center of the magnet. This results from the fact that the symmetry of the magnet around the xx and yy axes is very different and thus a large octupole term is produced, which in turn falls off slowly from the pole tip. The effect of the nonlinearity can easily be visualized as follows. The percentage deviation at any x is the percentage by which the angle of bend will be in error for a particle passing at

that x position, i.e., $\frac{x}{F + \Delta F}$, or its equivalent $\frac{x - \Delta x}{F}$, where F is the focal length. For example, for a 2% deviation at $x = 10''$ and for a parallel beam particle passing there, at the nominal focus F, the particle will be $0.200''$ off axis. The curves (Fig. 8) have been fitted to an octupole and 12 pole expansion as explained above and thus the expansion gives the same results (by definition) as Fig. 8 on the xx axis.

Consider the yy axis: the nonlinear terms will be the same magnitude as on the xx axis, but the phase of $4\theta/2\theta$ is opposite while the phase of $6\theta/2\theta$ is the same with respect to the xx axis. However, the real point of interest is that the maximum off-axis excursion is $3''$ as compared to $12''$ for the xx axis. Thus, the contribution of the small axis to the nonlinearity is negligible in comparison to the large axis' contribution.

Consider any position: for the small angles that one can go off the xx axis and still get to large values of x, the nonlinearity will be roughly that given in Fig. 8, for the same x value.

Thus, unless one is prepared to perform a very elaborate computation, considering the beam density distribution in two dimensions and reconstructing the field accordingly, the field can best be described by using Fig. 8 to give the deviation in B_y as a function of x not only on the xx axis, but also for off-axis positions. That is, the nonlinearity in B_y as shown in Fig. 8 (for $y = 0$) is roughly correct for all y values. Thus the nonlinearity calculation becomes a one dimensional problem and one needs only the incoming x-axis beam density distribution to calculate the aberration. If one is using most of the large aperture, the focal length at $x = 6''$ is roughly a mean. Fig. 9 gives the angle of bend at $x = 6''$ and thus $\langle F \rangle$. Dividing by L_B and $6''$, one gets $\langle G \rangle$, a mean

gradient strength for the lens about the xx axis. If less than the whole aperture is used one can interpolate from Fig. 8 and compute the appropriate $\langle G \rangle$ and $\langle F \rangle$ values.

VI. Conclusions

This report has presented working curves for both the circular and rectangular quadrupoles, which enable one to set up the lenses of a beam transport system. For the circular quadrupoles the coefficients and phase angles of terms in a harmonic expansion are listed, to high accuracy. From this data the nonlinearities can be treated completely in the thick lens approximation.

Absolute "spectrometer" curves are given for both the circular and rectangular quadrupoles.

For the rectangular quadrupoles, enough data is given to permit a complete expansion of the field in terms of the symmetrically allowed nonlinearities. In this case (unlike the circular quadrupoles) more general nonlinearities were not measured but the smoothness of the fit to the symmetrical nonlinearities shows that this restriction is not serious. A simple approach has been suggested wherein the aberration is considered as only one dimensional. For this approach, the error will be a fairly small part of the true aberration for reasonable beam density distributions, and it makes the analysis of the system much simpler.

ACKNOWLEDGEMENTS

The authors would like to thank Mr. J. Weisenbloom and Mr. G. Stenby who assisted in the magnetic measurements.

REFERENCE

1. G.T. Danby, Internal Report GTD-2, Accelerator Department, Brookhaven National Laboratory (December 1961).

GTD/JWJ/ejb

11/20/63

Distribution: AD B1, B2, B3

TABLE I Coefficients of Nonlinear Terms in Circular Quadrupole Field GTD/JMJ-2

R _m	Ratio of Coefficients		8024		8048		Scaling Factor	8024		8048		12030	12060	IX	Explanation of Column Headings
	I	II	III	IV	V	VI		VII	VIII						
Long Coil Measurements	5.4	48/28	0.17x10 ⁻³	0.66x10 ⁻³	1.031	11.0x10 ⁻³	8.59x10 ⁻³	0.17x10 ⁻³	0.61x10 ⁻³	I. Pole Tip Field (Kg).					
		68/28	10.71	8.33	1.063	3.31	3.60	12.43	8.96	II. Ratio of the coefficients of the nonlinear terms to the coefficient of the quadrupole term at the maximum radius of the harmonic coil (approx. 1/16 inch from the pole tip).					
		108/28	3.11	3.39	1.095	1.22	1.12	3.11	3.31	III. Ratio of the coefficients for an 8024 magnet.					
10.9		148/28	1.11	1.02				1.58	1.33	IV. Ratio of the coefficients for an 8048 magnet.					
		48/28	0.24x10 ⁻³	0.54x10 ⁻³	1.031	10.8x10 ⁻³	8.52x10 ⁻³	0.16x10 ⁻³	12.16	V. Numerical factors to be used in scaling the coefficients of an 8" diameter magnet to the same relative radius in a 12" dia. magnet.					
		68/28	10.51	8.26	1.063	3.08	3.50	2.78	4.95	VI. Ratio of the coefficients for an 8024 magnet scaled to a 12" diameter magnet.					
16.3		108/28	2.90	3.29	1.095	1.16	1.07	1.15	1.35	VII. Ratio of the coefficients for an 8048 magnet scaled to a 12" diameter magnet.					
		148/28	1.06	0.98						VIII. Ratio of the coefficients for a 12030 magnet.					
		48/28	0.24x10 ⁻³		1.031	9.7x10 ⁻³				IX. Ratio of the coefficients for a 12060 magnet.					
5.4		68/28	9.45		1.063	2.69									
		108/28	2.53		1.095	1.00									
		148/28	0.91												
Point Coil Measurements	5.4	48/28	0.11x10 ⁻³	1.13x10 ⁻³	1.031	5.77x10 ⁻³	5.84x10 ⁻³	0.04x10 ⁻³	0.12x10 ⁻³						
		68/28	5.60	5.66	1.063	4.42	4.41	4.42	4.65						
		108/28	4.16	4.15	1.095	1.38	1.40	1.28	1.33						
10.9		148/28	1.26	1.28											
		48/28	0.34x10 ⁻³	0.98x10 ⁻³	1.031	5.98x10 ⁻³	5.96x10 ⁻³	0.14x10 ⁻³	0.66x10 ⁻³						
		68/28	5.80	5.78	1.063	4.35	4.52	4.31	4.27						
16.3		108/28	4.09	4.25	1.095	1.32	1.39	1.17	1.35						
		148/28	1.21	1.27											
		48/28	0.40x10 ⁻³		1.031	7.32x10 ⁻³									
10.9		68/28	7.10		1.063	3.82									
		108/28	3.59		1.095	0.53									
		148/28	0.49												

NOTE: At the pole tip, the coefficients for 68 and 148 are in phase with the coefficient for 28, while the coefficient for 108 is out of phase with that for 28.

TABLE II Phase Angles of Harmonic Terms in Circular Quadrupole Field

GTD/JMJ-2

I R _k	II Harmonic Term	III Theoretical	IV 8024	V 8024 Difference	VI 8048	VII 8048 Difference	VIII 12030	IX 12030 Difference	X 12060	XI 12050 Difference
5.4	20	+45° 00'	+45° 04'	+00° 04'	+44° 58'	-0° 02'	+45° 00'	0° 00'	+45° 05'	+0° 05'
	40	-15° 00'	-21 45		-55 32		-6 14		+6 13	
	60	-9° 00'	-15 14	+	-15 32	+	-14 59	-	-15 04	+
	100	-6° 26'	-9 26	+	-9 17	+	-8 40	-	-8 52	-
	140		-6 28	+	-6 41	+	-6 06	-	-6 01	-
10.9	20	+45° 00'	+45° 20'	+0° 20'	+44° 40'	-0° 20'	+45° 01'	+0° 01'		
	40	-15° 00'	-13 21		-49 47		+2 42			
	60	-9° 00'	-15 07	+	-15 26	+	-14 56	-		
	100	-6° 26'	-8 56	+	-9 22	+	-8 41	-		
	140		-6 31	+	-6 50	+	-5 55	-		
10.3	20	+45° 00'	+44° 58'	-0° 02'						
	40	-15° 00'	-16 28							
	60	-9° 00'	-15 12	+						
	100	-6° 26'	-8 58	-						
	140		-6 20	-						
5.4	20	+45° 00'	+44° 57'	-0° 03'	+44° 44'	-0° 16'	+44° 51'	-0° 09'	+44° 46'	-0° 14'
	40	-15 00	-24 03		-52 42		-64 52		-2 06	
	60	-9 00	-15 44	+	-15 04	+	-15 06	+	-16 27	+1° 27'
	100	-6 26	-9 08	+	-9 12	+	-8 56	-	-8 52	- 08
	140		-6 25	+	-6 20	+	-6 00	-	-6 20	- 06
10.9	20	+45° 00'	+44° 57'	-0° 03'	+44° 52'	-0° 08'	+44° 51'	-0° 09'	+44° 45'	-0° 15'
	40	-15 00	-21 55		-49 29		-26 25		-7 21	
	60	-9 00	-15 42	+	-15 42	+	-15 07	+	-14 45	- 15
	100	-6 26	-9 09	+	-10 12	+	-8 55	-	-9 08	+ 08
	140		-6 32	+	-6 24	+	-5 41	-	-6 28	+ 02
16.3	20	+45° 00'	+44° 51'	-0° 09'						
	40	-15 00	-22 21							
	60	-9 00	-15 40	+						
	100	-6 26	-8 19	+						
	140		-6 19	+						

Explanation of Column Headings

- I. Pole tip field (K₂)
- II. Harmonic terms which exist in circularly symmetric quadrupole field (the 40 term is included since it is the largest of the asymmetrical terms).
- III. Theoretical phase angles which can be expected from the four pole symmetry.
- IV. Measured phase angles for an 8024 magnet.
- V. Deviation of 8024 measured phase angles from those predicted by four pole symmetry.
- VI to XI. Measured phase angles and their deviations for 8048, 12030 and 12060 magnets.

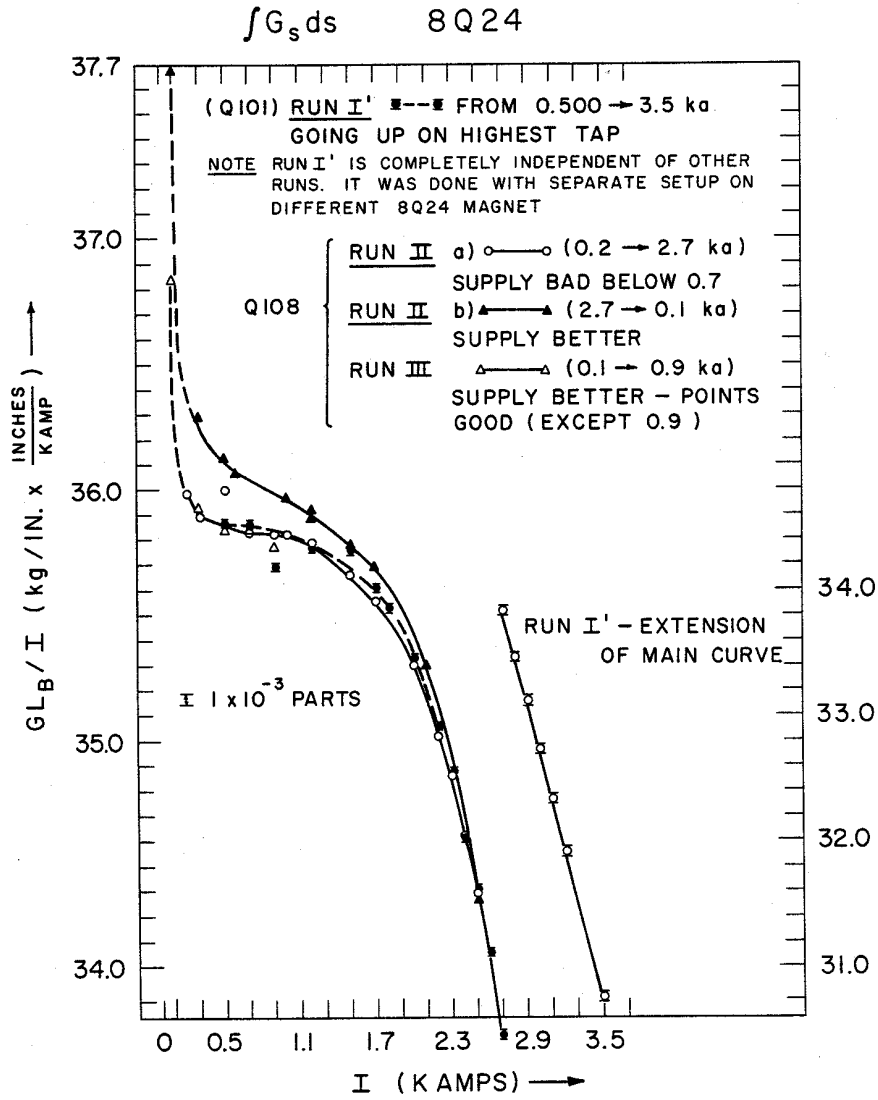


Figure 1. $\int G_s ds$ vs I for 8Q24 magnets.

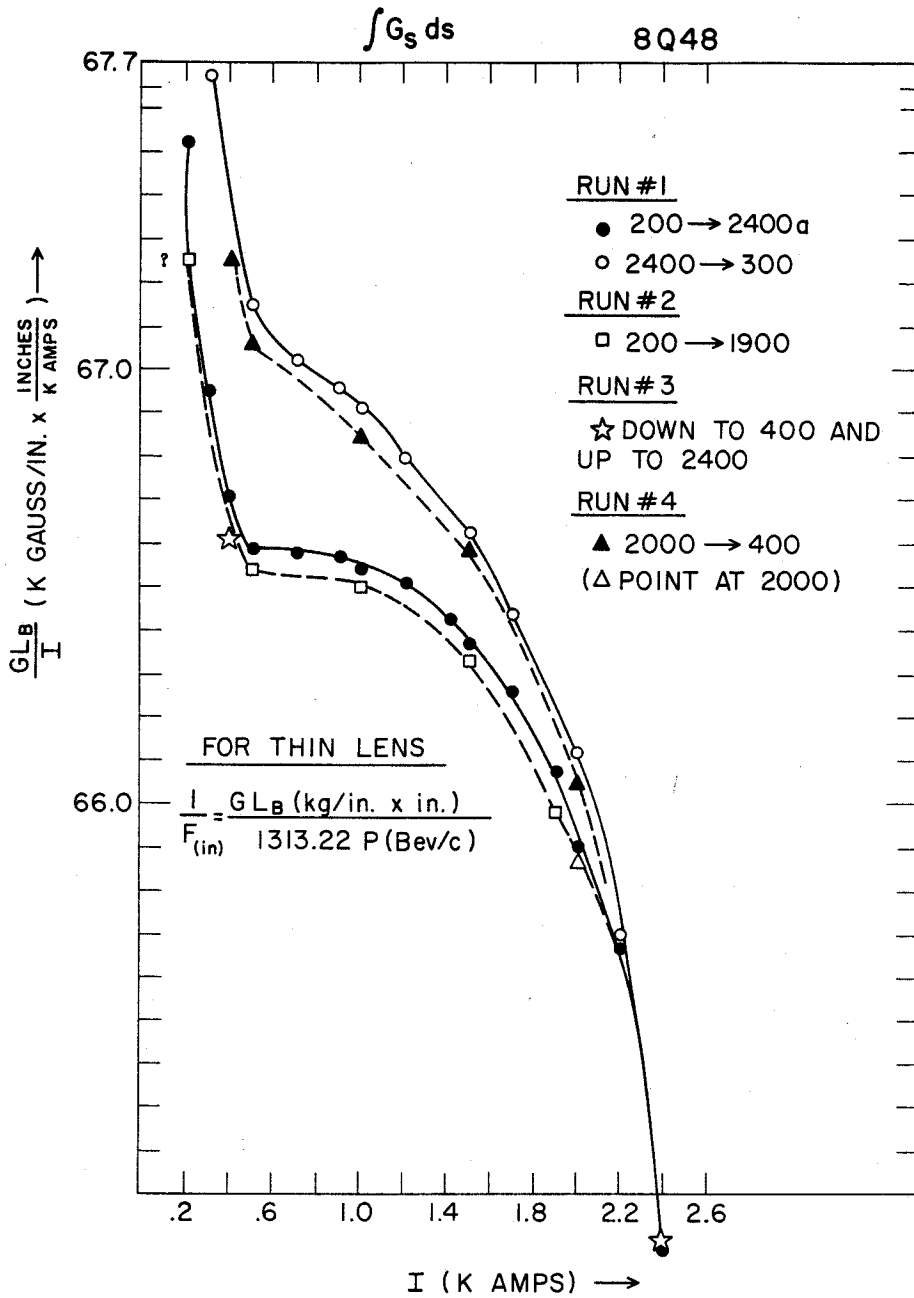


Figure 2. $\int G_s ds$ vs I for 8Q48 magnets.

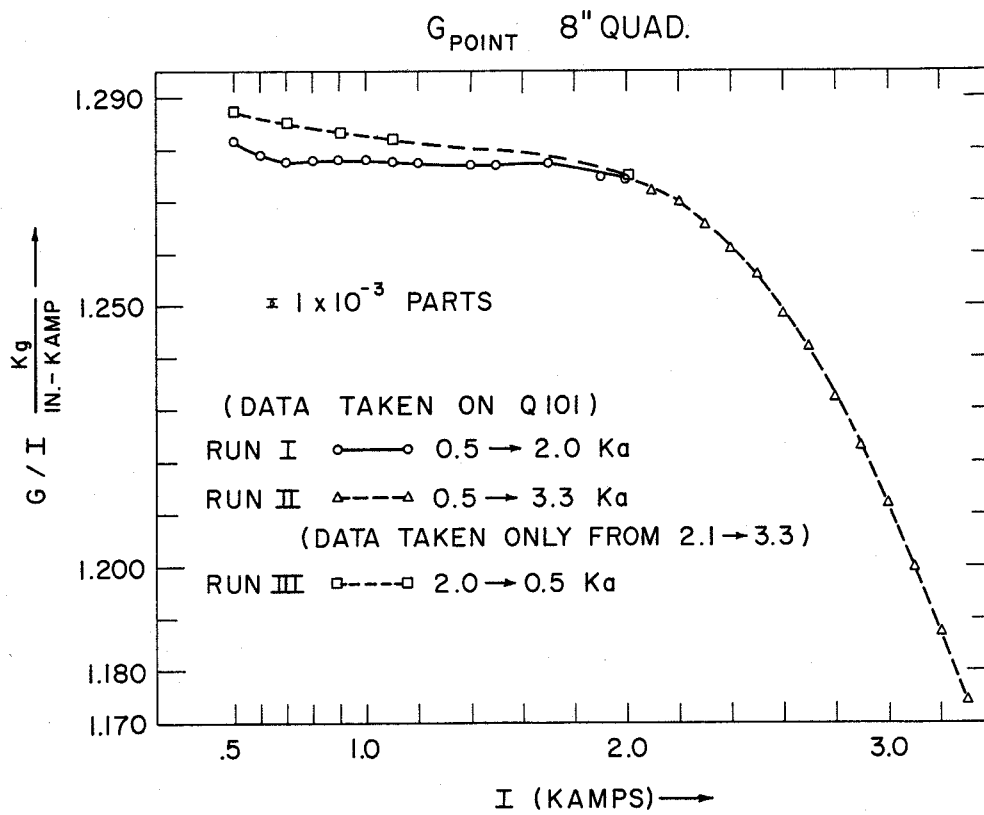


Figure 3. Gradient, G point, vs I for 8 inch quadrupoles.

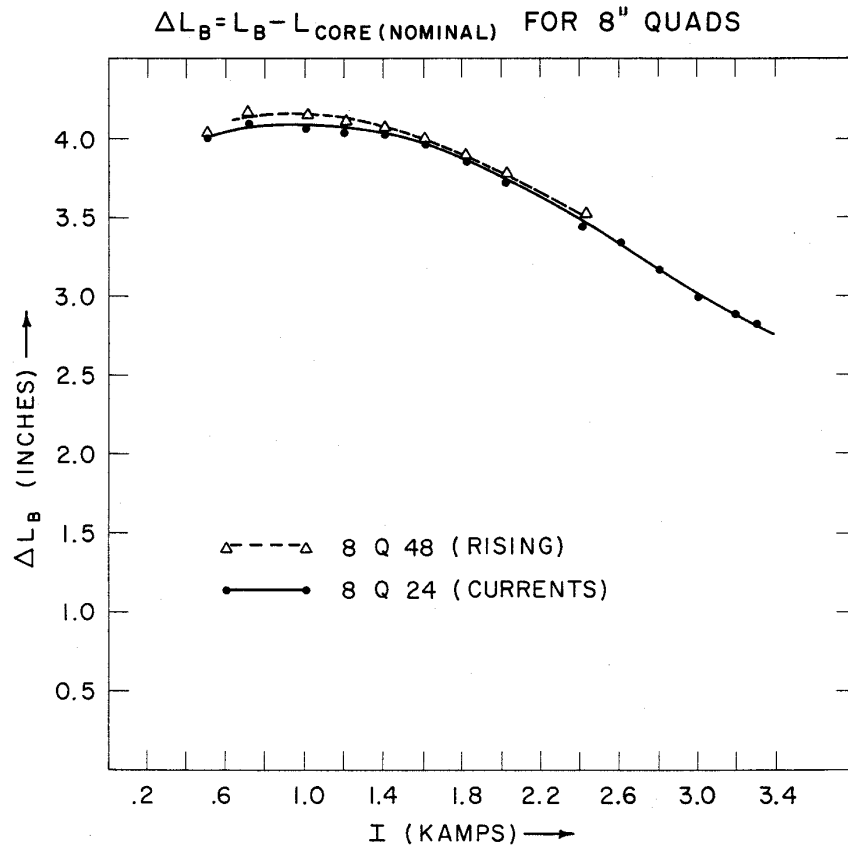


Figure 4. Magnet length, L_B , vs I for 8 inch quadrupoles. ($L_B = \Delta L_B + L_{core}$).

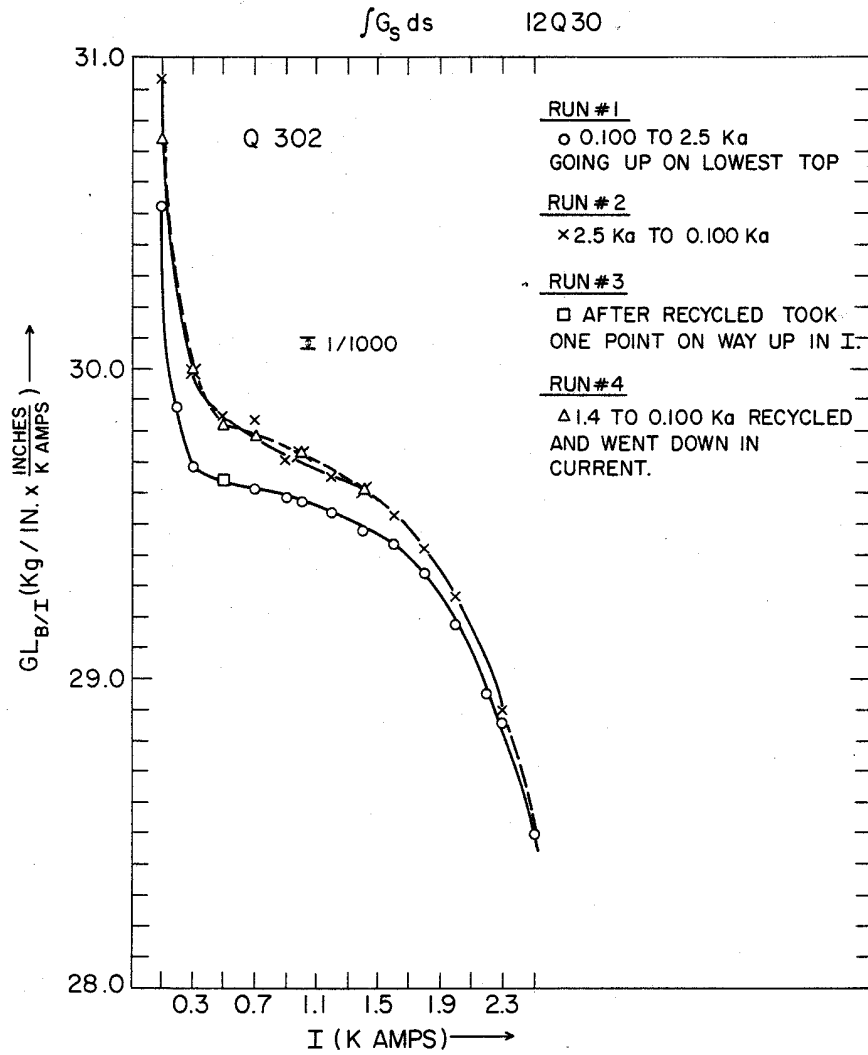


Figure 5. $\int G_s ds$ vs I for 12Q30 magnets.

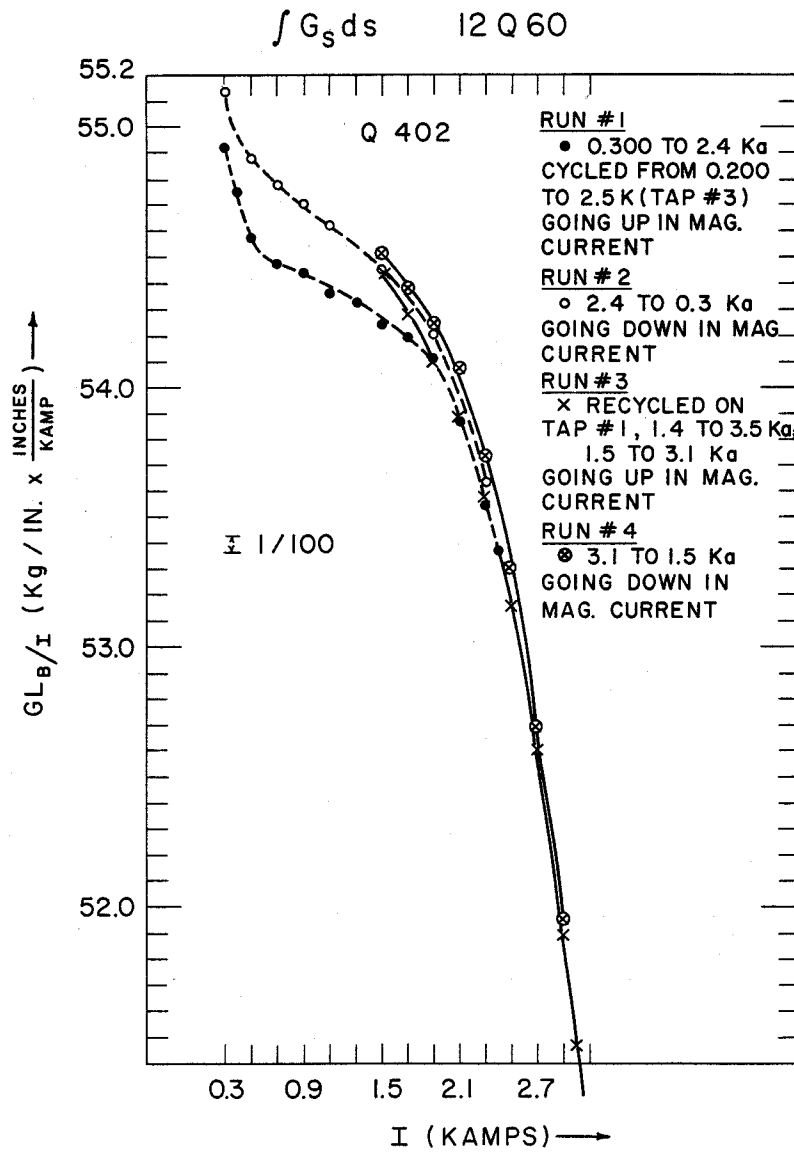


Figure 6. $\int G_s ds$ vs I for 12Q60 magnets.

AGS. RECTANGULAR QUADRUPOLE

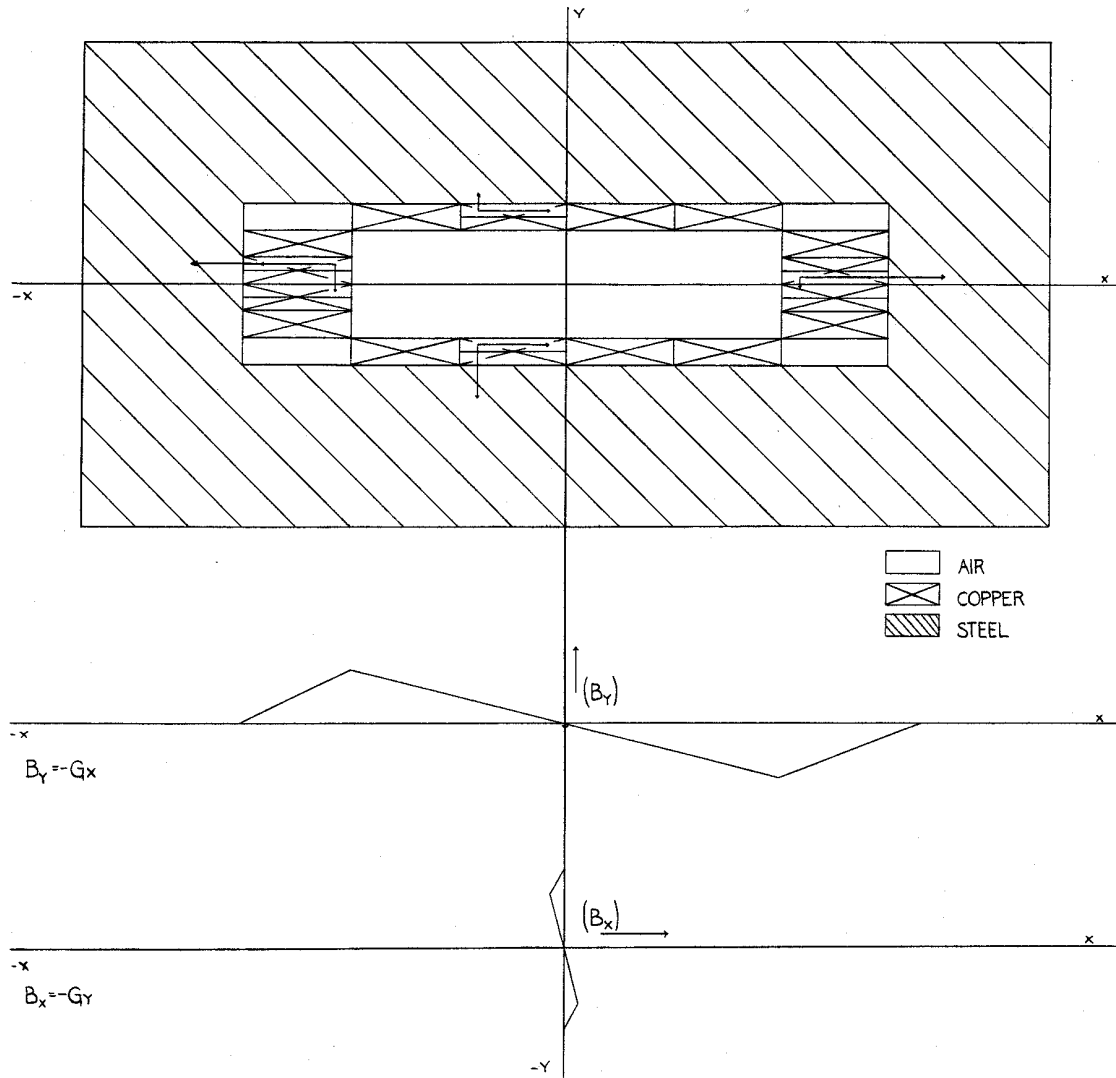


Figure 7

NONLINEARITY IN GRADIENT

R.Q. (6x24x36)

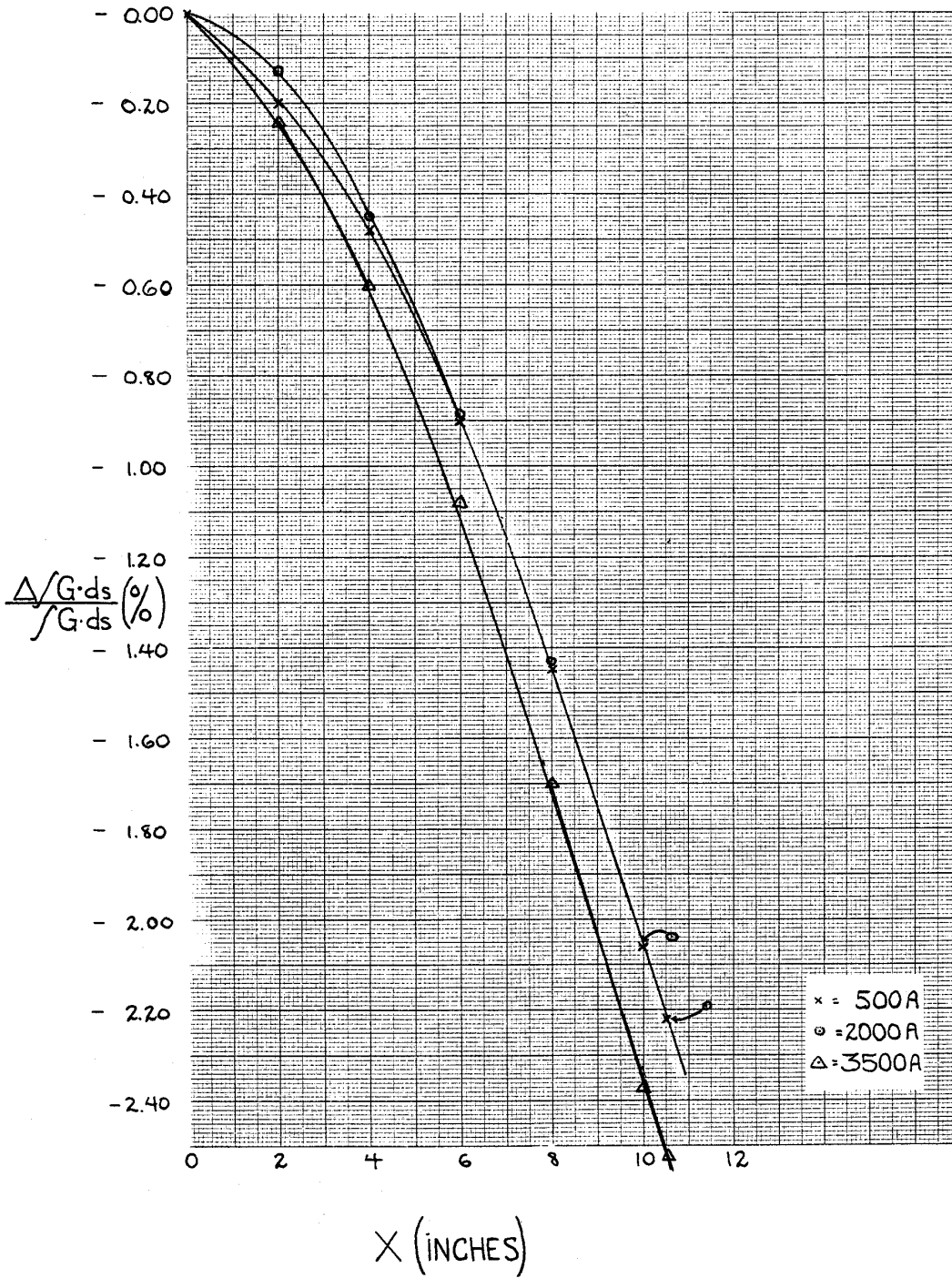


Figure 8

$$(\sin \theta_f - \sin \theta_i) P (B_{ev}/C) = \frac{1}{1313.22} \int B(s) ds (K_G - IN)$$

$$= \frac{BL_B (K_G - IN)}{1313.22} = \frac{6" G L_B}{1313.22}$$

R.Q.(6" x 24" x 36")

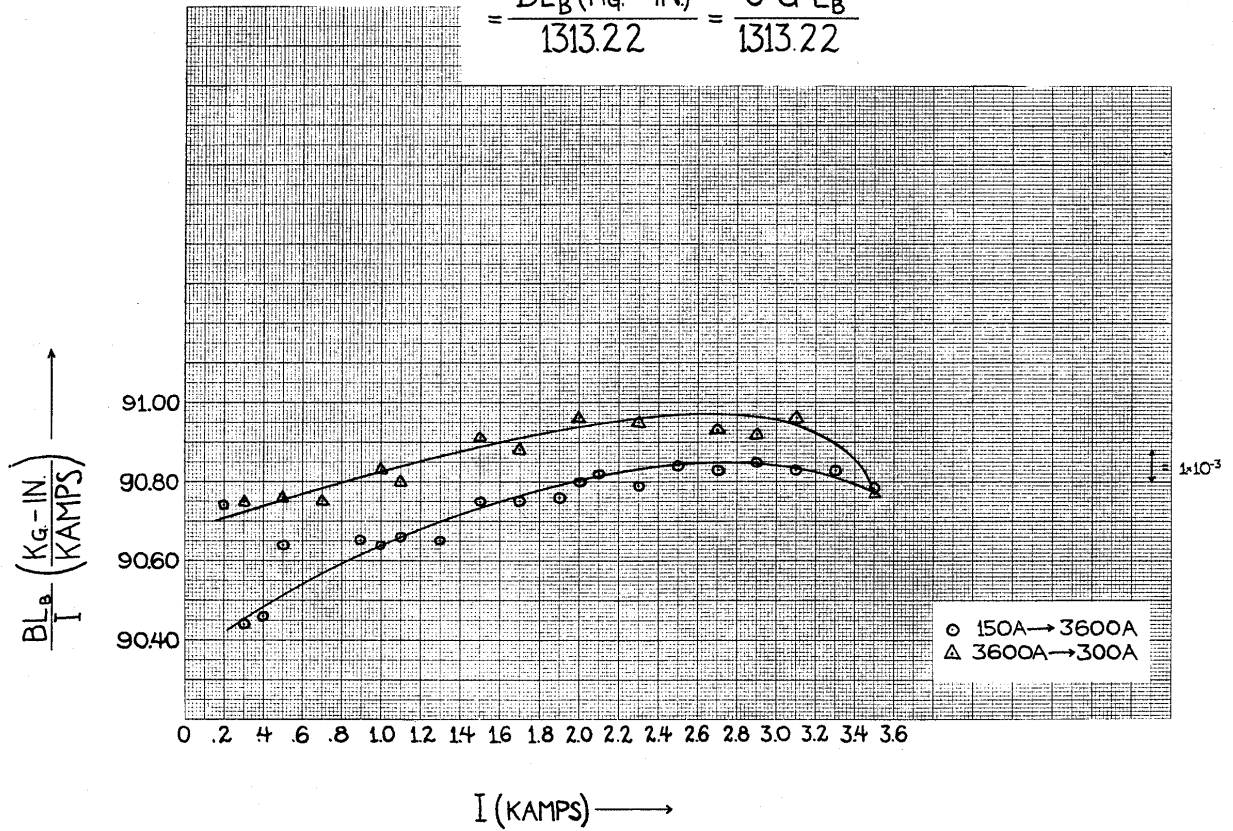


Figure 9

L_B vs I ($X=6''$)

R.Q. ($6'' \times 24'' \times 36''$)

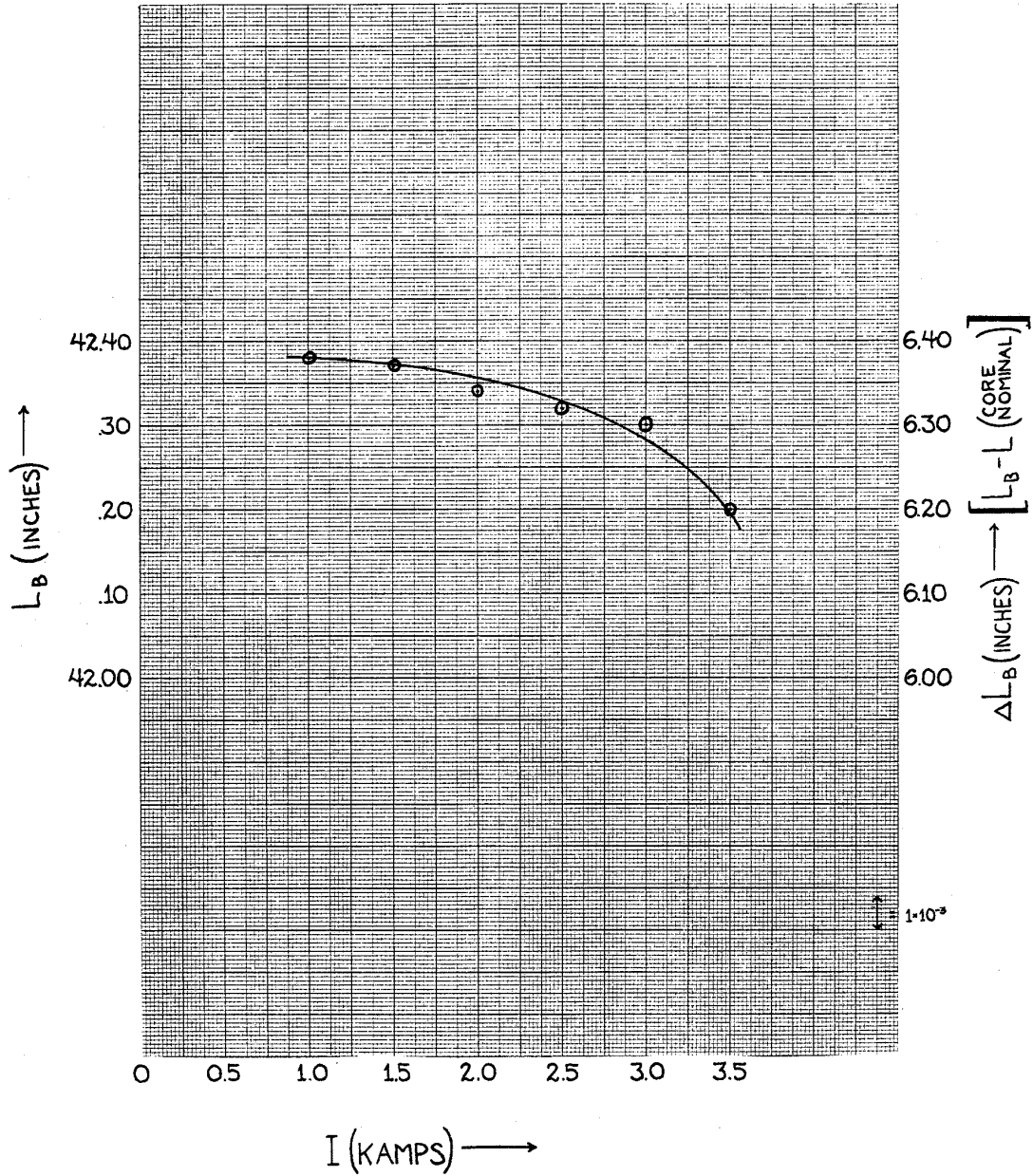


Figure 10